Check for updates

Circulation

ORIGINAL RESEARCH ARTICLE

Relationship of Subendocardial Perfusion to Myocardial Injury, Cardiac Structure, and Clinical Outcomes Among Patients With Hypertension

Xiaolei Xu, MD; Sanjay Divakaran, MD, MPH; Brittany N. Weber, MD, PhD; Jon Hainer, BS; Shelby S. Laychak, BS; Benjamin Auer, PhD; Marie Foley Kijewski, ScD; Ron Blankstein, MD; Sharmila Dorbala, MD, MPH; Ludovic Trinquart, PhD; Piotr J. Slomka, PhD; Li Zhang, MD, PhD*; Jenifer M. Brown, MD*; Marcelo F. Di Carli, MD*

BACKGROUND: Coronary microvascular dysfunction has been implicated in the development of hypertensive heart disease and heart failure, with subendocardial ischemia identified as a driver of sustained myocardial injury and fibrosis. We aimed to evaluate the relationships of subendocardial perfusion with cardiac injury, structure, and a composite of major adverse cardiac and cerebrovascular events consisting of death, heart failure hospitalization, myocardial infarction, and stroke.

METHODS: Layer-specific blood flow and myocardial flow reserve (MFR; stress/rest myocardial blood flow) were assessed by ^{13}N-ammonia perfusion positron emission tomography in consecutive patients with hypertension without flow-limiting coronary artery disease (summed stress score <3) imaged at Brigham and Women's Hospital (Boston, MA) from 2015 to 2021. In this post hoc observational study, biomarkers, echocardiographic parameters, and longitudinal clinical outcomes were compared by tertiles of subendocardial MFR ($MFR_{subendo}$).

RESULTS: Among 358 patients, the mean age was 70.6±12.0 years, and 53.4% were male. The median $MFR_{subendo}$ was 2.57 (interquartile range, 2.08–3.10), and lower $MFR_{subendo}$ was associated with older age, diabetes, lower renal function, greater coronary calcium burden, and higher systolic blood pressure ($P<0.05$ for all). In cross-sectional multivariable regression analyses, the lowest tertile of $MFR_{subendo}$ was associated with myocardial injury and with greater left ventricular wall thickness and volumes compared with the highest tertile. Relative to the highest tertile, low $MFR_{subendo}$ was independently associated with an increased rate of major adverse cardiac and cerebrovascular events (adjusted hazard ratio, 2.99 [95% CI, 1.39–6.44]; $P=0.005$) and heart failure hospitalization (adjusted hazard ratio, 2.76 [95% CI, 1.04–7.32; $P=0.042$) over 1.1 (interquartile range, 0.6–2.8) years median follow-up.

CONCLUSIONS: Among patients with hypertension without flow-limiting coronary artery disease, impaired $MFR_{subendo}$ was associated with cardiovascular risk factors, elevated cardiac biomarkers, cardiac structure, and clinical events.

Key Words: heart failure ■ hypertension ■ perfusion imaging ■ ventricular remodeling

Editorial, see p 1087

Downloaded from http://ahajournals.org by on March 29, 2025

Patients with hypertension and other states of pathologic hypertrophy may have symptoms and signs of myocardial ischemia despite the absence of obstructive coronary artery disease (CAD). Evidence suggests that coronary microvascular dysfunction, a cause of impaired myocardial oxygen supply, may play a pivotal role in symptoms and in the transition from adaptive to maladaptive left ventricular (LV) remodeling

Correspondence to: Marcelo F. Di Carli, MD, Brigham and Women's Hospital, ASB-L1 0370C, 75 Francis St, Boston, MA 02115. Email mdicarli@bwh.harvard.edu
*L. Zhang, J.M. Brown, and M.F. Di Carli contributed equally.
Supplemental Material, the podcast, and transcript are available with this article at https://www.ahajournals.org/doi/suppl/10.1161/CIRCULATIONAHA.123.067083.
For Sources of Funding and Disclosures, see page 1085.
© 2024 American Heart Association, Inc.
Circulation is available at www.ahajournals.org/journal/circ

Clinical Perspective

What Is New?

- Layer-specific subendocardial perfusion can be reliably quantified by ^{13}N-ammonia myocardial perfusion positron emission tomography and is correlated with cardiometabolic risk factors, cardiac injury, chamber dimensions, and clinical outcomes, thus capturing a physiologically relevant construct.

What Are the Clinical Implications?

- Quantification of subendocardial blood flow and flow reserve may be a promising tool for exploring the pathophysiology of hypertensive heart disease and heart failure in patients with hypertension.
- Whether subendocardial myocardial flow reserve will be able to provide unique prognostic information in patients with significant hypertrophy but preserved transmural myocardial flow reserve is not yet known.

Nonstandard Abbreviations and Acronyms

CAC	coronary artery calcium
CAD	coronary artery disease
HF	heart failure
hsTnT	high-sensitivity cardiac troponin T
LV	left ventricular
MACCE	major adverse cardiac and cerebrovascular events
MBF	myocardial blood flow
MFR	myocardial flow reserve
$MFR_{subendo}$	subendocardial myocardial flow reserve
MI	myocardial infarction
NT-proBNP	N-terminal pro-B-type natriuretic peptide
PET	positron emission tomography

in hypertensive heart disease.[1,2] Long-term elevated arterial blood pressure, overactivated neurohumoral systems, and increased inflammation and oxidative stress have been shown to be associated with LV hypertrophy and hypertensive heart failure (HF)[3,4] and may first yield abnormalities in perfusion of the subendocardial layer because of anatomic and functional abnormalities in the small vessels supplying this territory.

The coronary microvasculature is beyond the resolution of coronary angiography. Consequently, its clinical evaluation is necessarily indirect through the invasive or noninvasive quantification of coronary vasoreactivity.[5] Quantitative positron emission tomography (PET) imaging is considered the gold standard for the noninvasive assessment of myocardial blood flow (MBF) and myocardial flow reserve (MFR, ratio of stress/rest MBF).[6] However, the majority of previous studies have quantified MBF and MFR as transmural measures of tissue perfusion that are relatively insensitive to discrete abnormalities in perfusion of the subendocardium, which is more vulnerable to ischemic injury because of the heterogeneity of the coronary microcirculation.[7,8] Although previous studies have performed PET quantification of subendocardial perfusion in healthy volunteers[9] and patients with obstructive epicardial CAD[10] and hypertrophic cardiomyopathy,[11,12] they have not related subendocardial ischemia to clinical outcomes. To our knowledge, the 1 study to have evaluated the relationship of subendocardial perfusion to outcomes did not identify a relationship to atherosclerotic events; however, HF, a highly relevant outcome to subendocardial ischemia, was not assessed.[8] Given the technical challenges of layer-specific quantification, linking subendocardial blood flow to pertinent clinical end points would provide important evidence of the validity of subendocardial perfusion assessment.

To interrogate the pathophysiologic and prognostic significance of subendocardial layer-specific perfusion, we studied a cohort of patients with hypertension undergoing rest/stress PET perfusion imaging but without overt obstructive CAD to assess the quantitative relationship between subendocardial myocardial perfusion, cardiac structure, and clinical outcomes. We hypothesized that subendocardial MFR ($MFR_{subendo}$) would be associated with subclinical myocardial injury, alterations in LV structure, and clinical adverse cardiovascular events including HF hospitalization.

METHODS

Data supporting the findings of this study can be made available upon reasonable request to the corresponding author. This report adheres to the STROBE (Strengthening the Reporting of Observational Studies in Epidemiology) reporting guidelines for observational studies.

Study Design and Patients

Cross-sectional and longitudinal analyses were specified post hoc and performed to evaluate the pathophysiologic significance of subendocardial perfusion. The study population included patients with a clinical diagnosis of hypertension who underwent rest/stress myocardial perfusion PET imaging at Brigham and Women's Hospital (Boston, MA) between December 1, 2015, and December 1, 2021, without overt flow-limiting CAD[13] (defined as summed stress score <3 on standard 17-segment assessment,[14] indicating normal myocardial perfusion), who also underwent 2-dimensional echocardiography within 60 days of the PET scan, to facilitate comparisons of subendocardial perfusion and cardiac structure and function. Derivation of the patient cohort is shown in Figure S1. Sample size was not prespecified. Of 422 patients with hypertension who underwent perfusion PET and echocardiography within 60 days during the 6-year period, patients with a history of

Downloaded from http://ahajournals.org by on March 29, 2025

previous coronary artery bypass grafting or heart transplantation were excluded, as were those with compromised image quality that precluded accurate segmental analysis (5.2%). Patients with a reduced ejection fraction or history of previous percutaneous coronary intervention but with normal perfusion scan were included. The study was approved by the Mass General Brigham Institutional Review Board, and informed consent was waived in accordance with institutional guidelines.

Assessment of Circulating Biomarkers

Biomarkers of myocardial injury and stress within 90 days of the date of the PET scan, including hsTnT (high-sensitivity cardiac troponin T) and NT-proBNP (N-terminal pro-B-type natriuretic peptide), were obtained from the clinical medical records. hsTnT and NT-proBNP were measured by electrochemiluminescence immunoassay (Elecsys Troponin T Gen 5 STAT and Elecsys proBNP II, Roche Diagnostics, Indianapolis, IN). For hsTnT, the lower limit of quantitation was 6 ng/L, and the upper reference limit of 19 ng/L[15] was used to define a categorically elevated hsTnT. Sensitivity analyses for the upper reference limit were performed using the clinically reported cutoffs in our health care system (values >9 ng/L for female patients and >14 ng/L for male patients). For NT-proBNP, the lower limit of quantitation was 5 pg/mL. An upper reference limit of 300 pg/mL[16] was used to define a categorically elevated NT-proBNP. Sensitivity analyses for the upper reference limit were performed using the clinically reported cutoffs of 450, 900, or 1800 pg/mL depending on patient age and clinical site. In case of repeated measurements, the one with the shortest interval from the PET scan was selected. Estimated glomerular filtration rate (eGFR) was calculated from the serum creatinine using the 2021 Chronic Kidney Disease Epidemiology Collaboration formula.[17]

Assessment of LV Function and Structure

LV mass, LV end-diastolic volume, and LV end-systolic volume were obtained from the gated PET myocardial perfusion images. Indexed LV mass, end-diastolic volume, and end-systolic volume were calculated by dividing each parameter by the body surface area. LV posterior wall thickness, interventricular septal wall thickness, LV ejection fraction, and E/A ratio were quantified from the 2-dimensional echocardiograms by experienced clinical operators blinded to the research study questions.

Segmentation and Quantification of Subendocardial Blood Flow

All patients underwent myocardial perfusion PET on a whole-body PET/computed tomography scanner (GE Discovery RX or MI, Waukesha, WI) with a spatial resolution of 2 to 5 mm. ^{13}N-ammonia was used as the flow tracer. Myocardial perfusion images were obtained at rest and at peak hyperemic stress after intravenous regadenoson administration as per standard protocol. A low-dose noncontrast computed tomography scan was used for attenuation correction of the myocardial perfusion images. A research version of QPET (Cedars-Sinai, Los Angeles, CA) was used for layer-specific segmentation and blood flow quantification. Automatic motion correction with frame-by-frame manual adjustment was applied to all dynamic studies. The myocardium was then segmented using a standard QPET algorithm on summed dynamic images (skipping the first 2 minutes of these images), as previously described.[18] The contour of the myocardium defined from these summed images was then applied to all frames of the dynamic acquisition. This process outlines both the outer (epicardial) and inner (endocardial) surfaces of the myocardium. After this, a midsurface is automatically created, located precisely between the epicardial and endocardial surfaces by standard geometric sampling. This midsurface acts as a boundary for the subendocardial counts. Subsequently, the subendocardial counts are obtained from the part of the myocardium that lies between the inner (endocardial) surface and this midsurface. This results in segmentation of the LV wall into 2 layers of approximately equal thickness; the inner ring was defined as subendocardium, and the outer ring as subepicardium. Representative polar maps demonstrating layer-specific myocardial blood flow and flow reserve are shown in Figure 1. A small region of interest was placed in the left atrium to ascertain the arterial blood input function. The corresponding transmural, subendocardial, and subepicardial tissue time-activity curves were fitted to a 2-compartment kinetic model[18] to obtain layer-specific absolute MBF at rest and at stress in mL/min•g. To minimize partial volume effects, the spillover fraction was estimated as a model parameter. MFR was calculated as the ratio of stress over rest MBF.

Assessment of Coronary Calcification Scoring

In approximately one-third of cases, dedicated gated cardiac computed tomography for coronary artery calcium (CAC) scoring (collimation, 64 × 0.625 mm; gantry rotation time, 350 ms; effective temporal resolution, 175 ms; 120 kVp; 300 mA) was obtained as per standard care and used to calculate the Agatston score (Visage Imaging Inc, San Diego, CA). Agatston scores were categorized as none to mild (0–100), moderate (100–1000), or severe (>1000) calcification. In the remainder of cases, CAC scoring was evaluated by semiquantitative visual assessment of the transmission computed tomography scan by an experienced reader blinded to clinical and myocardial perfusion imaging data. Semiquantitative CAC assessment was categorized as none to mild, moderate, or severe, as previously described.[19,20] To verify accuracy, visual assessment was performed in the 113 cases with clinically performed CAC scoring and demonstrated excellent agreement (weighted kappa, 0.80 [95% CI, 0.71–0.89]) with 85.0% assigned to the matching category and 100% within 1 category of that assigned based on quantitative Agatston score. Adjudication by a second physician was used for any borderline cases.

Clinical Outcomes

The primary clinical outcome was a composite of major adverse cardiac and cerebrovascular events (MACCE), defined as the time to the first event among HF hospitalization, nonfatal myocardial infarction (MI), nonfatal stroke, or all-cause death. Secondary outcomes included the individual components of the primary composite end point. Clinical adjudication was conducted by reviewing the electronic medical record. Cause of death and hospitalization were determined by 2 separate physicians, blinded to myocardial perfusion data, with a third physician consulted if there were any uncertainties. MI was defined according to the "Fourth Universal Definition of Myocardial Infarction" (2018), including ST–elevation and non–ST–elevation MI.[21]

Downloaded from http://ahajournals.org by on March 29, 2025

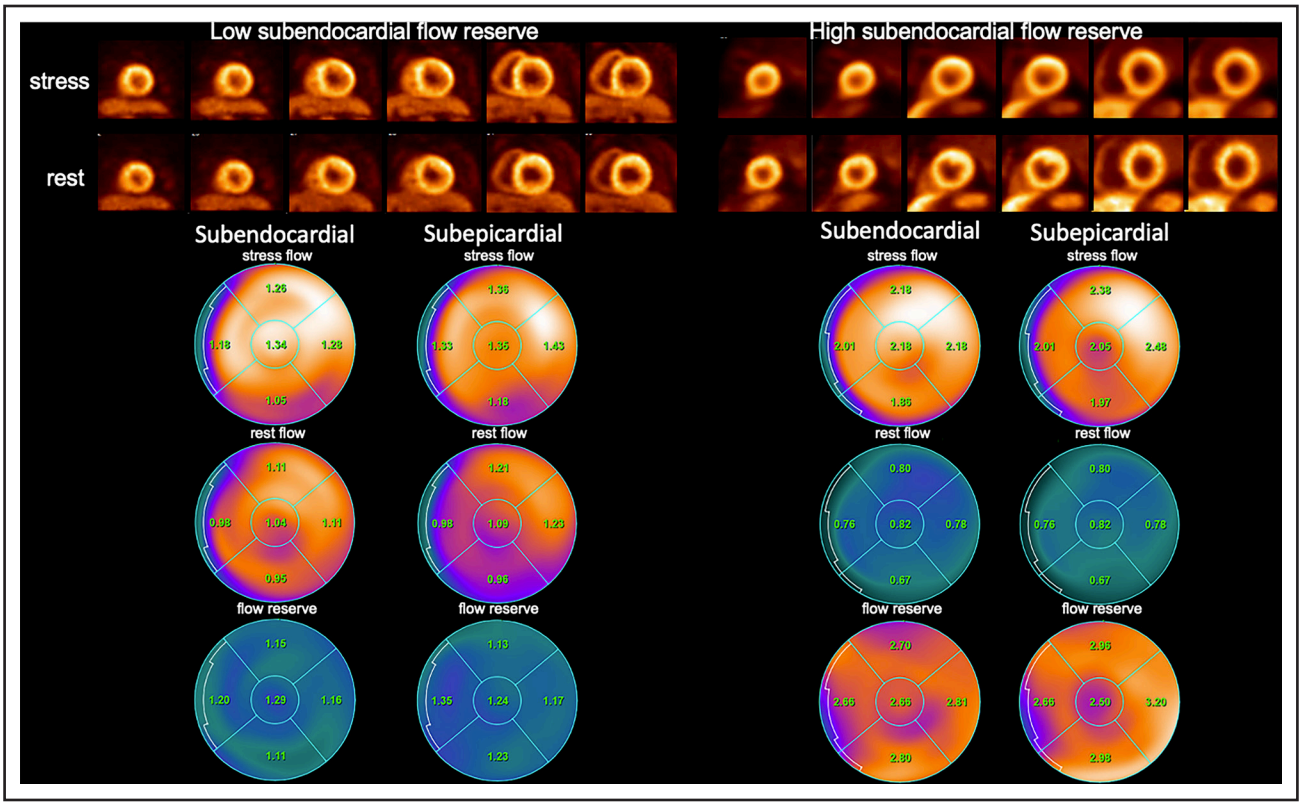

Figure 1. Layer-specific myocardial blood flow and flow reserve.
Top, Selected short-axis views of stress and rest myocardial perfusion positron emission tomography images of 2 patients without obstructive coronary artery disease showing low (**left**) and high (**right**) subendocardial flow reserve. The images on the **left** show mild transient left ventricular cavity dilatation during stress resulting from concentric subendocardial ischemia. **Bottom**, Corresponding parametric polar maps of stress and rest subendocardial and subepicardial myocardial blood flow (in mL/min•g of myocardium) and flow reserve (ratio of stress over rest myocardial blood flow).

Downloaded from http://ahajournals.org by on March 29, 2025

Stroke included ischemic and hemorrhagic stroke, diagnosed by the combination of symptoms, signs, and imaging results.[22] HF hospitalization was defined when a patient was discharged with a primary hospitalization diagnosis of HF, or with the clinical symptoms/signs of HF or elevated natriuretic peptide and initiation or intensification of HF-directed therapy (eg, diuretics).[23] Patients without clinical events were censored on the date of adjudication if last chart contact was within 6 months from adjudication; otherwise, the date of last contact was used.

Statistical Analysis

Mean±SD or median (interquartile range) are reported for continuous variables, and categorical variables are presented as counts and percentages. Interobserver reproducibility between 2 trained readers was evaluated with the average intraclass correlation coefficient with a 2-way mixed-effects model for absolute agreement on 20 test cases. Patients were categorized into tertiles of $MFR_{subendo}$. We tested for trends in baseline characteristics across tertile groups of $MFR_{subendo}$ by using the Jonckheere-Terpstra test.

Univariable and multivariable-adjusted associations between $MFR_{subendo}$ and elevated markers of myocardial injury, above the upper reference limit, were evaluated by logistic regression models. Linear regression models were used to assess the relationship of $MFR_{subendo}$ with indices of LV systolic and diastolic function and LV structure (wall thickness and chamber volumes). We report 2 adjusted models: model 1 was adjusted for age, sex, diabetes, and eGFR; model 2 was further adjusted for the burden of atherosclerosis by semiquantitative CAC scoring (none/mild, moderate, severe). Covariates were selected on the basis of previous evidence of their relevance to myocardial perfusion, injury, and remodeling and to clinical outcomes. Missing data occurred in some of our dependent variables (NT-proBNP, hsTnT, interventricular septal wall thickness, posterior wall thickness, echocardiographic LV ejection fraction, and E/A ratio), and complete cases for each dependent variable were analyzed.

Unadjusted Kaplan-Meier curves were generated for time to first MACCE and compared between $MFR_{subendo}$ tertile groups with the log-rank test. The association between MACCE and $MFR_{subendo}$ was assessed further by multivariable Cox proportional hazards models. The proportional hazards assumption was assessed by inspecting Schoenfeld residuals. Variables included for adjustment were age, sex, diabetes, eGFR, and CAC score, with an additional model further adjusting for mean LV wall thickness and LV ejection fraction. In secondary analyses, we evaluated the relationship between peak stress subendocardial blood flow, rather than flow reserve, and MACCE. We repeated these Cox model analyses for MACE (first event of HF hospitalization, MI, or death) and for time to all-cause death. For the individual component nonfatal events (time to HF hospitalization, time to nonfatal MI, time to nonfatal stroke), we used cause-specific proportional hazards models to assess the

relative effect of $MFR_{subendo}$ on the rate of occurrence of each nonfatal event among subjects who are currently event-free.[24]

Two-sided *P* values <0.05 were considered as statistically significant. All statistical analyses were performed with RStudio (2021.09.1, Build 372, RStudio, PBC, Boston, MA) and SAS 9.4 (SAS Institute, Cary, NC).

RESULTS

Baseline Characteristics

The baseline characteristics of the overall cohort (n=358) are shown in Table 1. The study cohort had a mean age of 70.6±12.0 years, and 191 (53.4%) were male, with average body mass index 31.6±7.6 kg/m^2. Evaluation of chest pain and of dyspnea were the most common reasons for referral to PET myocardial perfusion imaging. The study cohort had a median LV ejection fraction of 60%, with relatively normal LV thickness (median interventricular septal wall thickness, 11 mm; and posterior wall thickness, 10 mm). The median NT-proBNP was 549 (128–2148) pg/mL (n=209), with 132 (63.2%) above the upper reference limit. The median interval between PET and NT-proBNP measurement was 5.5 (1.9–24.4) days. The median hsTnT was 22.0 (11.0–55.5) ng/L (n=155), with 150 (96.8%) detectable and 109 (70.3%) above the upper reference limit. The median interval between PET and hsTnT measurement was 4.0 (1.5–22.6) days.

Association Between $MFR_{subendo}$ and Cardiovascular Risk Factors, Myocardial Injury, and LV Functional and Structural Abnormalities

The distributions of subendocardial and transmural myocardial blood flow and flow reserve are shown in Figure S2. Quantification of rest and stress subendocardial blood flow and flow reserve were highly reproducible, with an intraclass correlation coefficient ≥0.93 (95% CI, 0.83–0.97). Patients in the lowest tertile of $MFR_{subendo}$ were older and more likely to have diabetes and chronic kidney disease (Table 2). There was a stepwise increase in circulating hsTnT and NT-proBNP levels with decreasing $MFR_{subendo}$ (Figure 2). Likewise, patients in lower tertiles of $MFR_{subendo}$ had more abnormal chamber dimensions, with larger LV volumes and greater LV wall thickness (Figure 3). Interestingly, despite normal global LV myocardial perfusion, lower $MFR_{subendo}$ was also associated with more severe coronary calcification (Table 2).

In multivariable modeling, low $MFR_{subendo}$ was independently associated with elevated hsTnT and NT-proBNP (Table 3; Tables S1 and S2). Conversely, lower absolute resting subendocardial blood flow was associated with lower odds of an elevated hsTnT and was not associated with NT-proBNP elevation. Lower peak stress subendocardial blood flow was associated with higher odds of elevated NT-proBNP and was not associated with ele-

Table 1. Baseline Characteristics

Baseline characteristics	Cohort n=358
Demographics	
Age, y	70.6±12.0
Male, n (%)	191 (53.4)
BMI, kg/m^2	31.6±7.6
Cardiovascular risk factors, n (%)	
Hypertension	358 (100)
Dyslipidemia	287 (80.2)
Diabetes	131 (36.6)
CAD	90 (25.1)
Medications, n (%)	
Beta-Blockers	250 (69.8)
Calcium channel blockers	138 (38.6)
ACE inhibitor/ARB	192 (53.6)
Diuretics	161 (45.0)
Lipid-lowering therapies	285 (79.6)
Aspirin	216 (60.3)
Insulin	85 (23.7)
Symptoms, n (%)	
Chest pain	141 (39.4)
Dyspnea	153 (42.7)
Chest pain and dyspnea	33 (9.2)
Others	97 (27.1)
Left ventricular structure and function	
By echocardiography	
LVIDed, mm, n=349	45.0 [40.0–50.0]
LVIDes, mm, n=348	30.0 [26.0–35.0]
IVS, mm, n=349	11.0 [10.0–13.0]
PWT, mm, n=349	10.0 [9.0–12.0]
LVEF (%), n=354	60.0 [51.3–65.0]
E/A ratio, n=310	0.94 [0.77–1.28]
By PET	
Rest EDVi, mL/m^2	59.4 [48.5–75.7]
Stress EDVi, mL/m^2	63.3 [52.0–80.4]
Rest ESVi, mL/m^2	25.0 [18.4–37.4]
Stress ESVi, mL/m^2	26.1 [19.2–40.1]
LVMI, g/m^2	76.0 [68.0–87.0]
Laboratory tests	
NT-proBNP, pg/mL, n=209	549 [128–2148]
hsTnT, ng/L, n=155	22.0 [11.0–55.5]
eGFR, mL/min•1.73 m^2, n=346	65.3 [43.8–83.9]
HbA1c, %, n=275	6.0 [5.6–6.8]

Values are shown as n (%), mean±SD, or median [interquartile range]. Laboratory parameters were available in a subset of the total study population: NT-proBNP n=209, hsTnT n=155, eGFR n=346, HbA1c n=275. Lipid-lowering therapies include statins, ezetimibe, and PCSK9 (proprotein convertase subtilisin/kexin type 9) inhibitors. ACE indicates angiotensin-converting enzyme; ARB, angiotensin receptor blocker; BMI, body mass index; EDVi, end-diastolic volume index; ESVi, end-systolic volume index; eGFR, estimated glomerular filtration rate; HbA1c, hemoglobin A1c; hsTnT, high-sensitivity cardiac troponin T; IVS, interventricular septal wall thickness; LVEF, left ventricular ejection fraction; LVIDed, left ventricular internal dimension at end-diastole; LVIDes, left ventricular internal dimension at end-systole; LVMI, left ventricular mass index; NT-proBNP, N-terminal pro-B-type natriuretic peptide; PET, positron emission tomography; and PWT, posterior wall thickness.

Downloaded from http://ahajournals.org by on March 29, 2025

Table 2. Association of Subendocardial MFR With Cardiovascular Risk Factors and Atherosclerosis

	$MFR_{subendo}$ tertile group 1 n=120	$MFR_{subendo}$ tertile group 2 n=119	$MFR_{subendo}$ tertile group 3 n=119	Trend *P* value
Subendocardial MFR	1.81±0.33	2.57±0.18	3.48±0.44	n/a
Age, y	73.5±12.6	72.5±10.3	65.8±11.5	<0.001
Male, n (%)	66 (55.0%)	65 (54.6%)	60 (50.4%)	0.27
BMI, kg/m^2	30.8±8.0	31.3±6.7	32.7±7.8	0.016
History of DM, n (%)	58 (48.3%)	42 (35.3%)	32 (26.9%)	0.003
History of dyslipidemia, n (%)	106 (88.3%)	95 (79.8%)	86 (72.3%)	0.016
History of CAD, n (%)	29 (24.2%)	33 (27.7%)	28 (23.5%)	0.93
History of PCI, n (%)	20 (16.7%)	26 (21.9%)	22 (18.5%)	0.81
eGFR, mL/min•1.73 m^2 n=346	51.7±27.4	66.3±24.5	71.2±22.5	<0.001
HbA1C, n (%) n=275	6.6±1.5	6.7± 2.3	6.1±1.2	0.002
Rest SBP, mm Hg	146±26	141±23	139±22	0.013
Rest DBP, mm Hg	74±13	73±12	73±12	0.48
Rest HR, bpm	74±15	70±11	68±13	0.001
CAC score				
None to mild	41 (34.2%)	57 (47.9%)	68 (57.1%)	<0.001
Moderate	30 (25.0%)	26 (21.8%)	31 (26.1%)	
Severe	49 (40.8%)	36 (30.3%)	20 (16.8%)	
Transmural MFR	1.84±0.35	2.61±0.25	3.40±0.49	<0.001
Subendo stress MBF, mL/min•g	1.73±0.47	2.01±0.46	2.15±0.47	<0.001
Subendo rest MBF, mL/min•g	0.98±0.26	0.79±0.18	0.64±0.14	<0.001

Lower subendocardial MFR ($MFR_{subendo}$) was associated with older age, more prevalent diabetes, lower renal function, greater coronary calcium, and higher systolic blood pressure. The median $MFR_{subendo}$ was 2.57 [interquartile range, 2.08–3.10]. *P* values for trend across tertile groups of $MFR_{subendo}$ are based on the Jonckheere-Terpstra test. CAC indicates coronary artery calcium; CAD, coronary artery disease; DBP, diastolic blood pressure; DM, diabetes mellitus; eGFR, estimated glomerular filtration rate; HbA1c, hemoglobin A1c; HR, heart rate; MBF, myocardial blood flow; PCI, percutaneous coronary intervention; and SBP, systolic blood pressure.

vated hsTnT. In linear regression models, lower $MFR_{subendo}$ was associated with increased LV volumes, mass, and wall thickness (Table 4; Table S2), and consistent associations with structural parameters were observed with absolute peak stress subendocardial blood flow (Table S3). Conversely, lower absolute resting subendocardial blood flow was not independently associated with LV volumes, wall thickness, or mass.

Association Between $MFR_{subendo}$ and Adverse Clinical Outcomes

After a median follow-up of 1.1 (0.5–2.7) years, a total of 82 MACCE events occurred in 69 patients, including 28 deaths, 4 MIs, 12 strokes, and 38 HF hospitalizations (Table S4). In multivariable Cox regression modeling, lower $MFR_{subendo}$ was independently associated with increased rate of MACCE after adjustment for age, sex, diabetes, CAC score, eGFR, mean wall thickness, and LV ejection fraction (adjusted HR in lowest versus highest tertile groups, 2.99 [95% CI, 1.39–6.44]; *P*=0.005). Kaplan-Meier curves also showed a stepwise relationship between lower $MFR_{subendo}$ and worse prognosis (Figure 4). In secondary analyses, low $MFR_{subendo}$ was also associated with an increased rate of HF hospitalization and with all-cause death, although the association with death was no longer significant after adjusting for covariates (Table 5). Similarly, lower peak stress subendocardial blood flow was associated with a higher rate of adverse clinical outcomes and with HF hospitalization, although the effect was attenuated in the fully adjusted model (Table S5). The ratio of subendocardial to subepicardial blood flow was evaluated; resting subendocardial flow was 97.1%±7.6% of subepicardial flow, and with maximal hyperemic stress, there was an expected decline in the ratio of subendocardial to subepicardial flow, although this ratio was not predictive of structural cardiac parameters or clinical outcomes. As expected, given the strong correlation between transmural and subendocardial MFR in this population, $MFR_{subendo}$ did not provide additive prognostic information to transmural MFR.

DISCUSSION

We found that lower $MFR_{subendo}$ is associated with increased cardiovascular risk factors including diabetes

Downloaded from http://ahajournals.org by on March 29, 2025

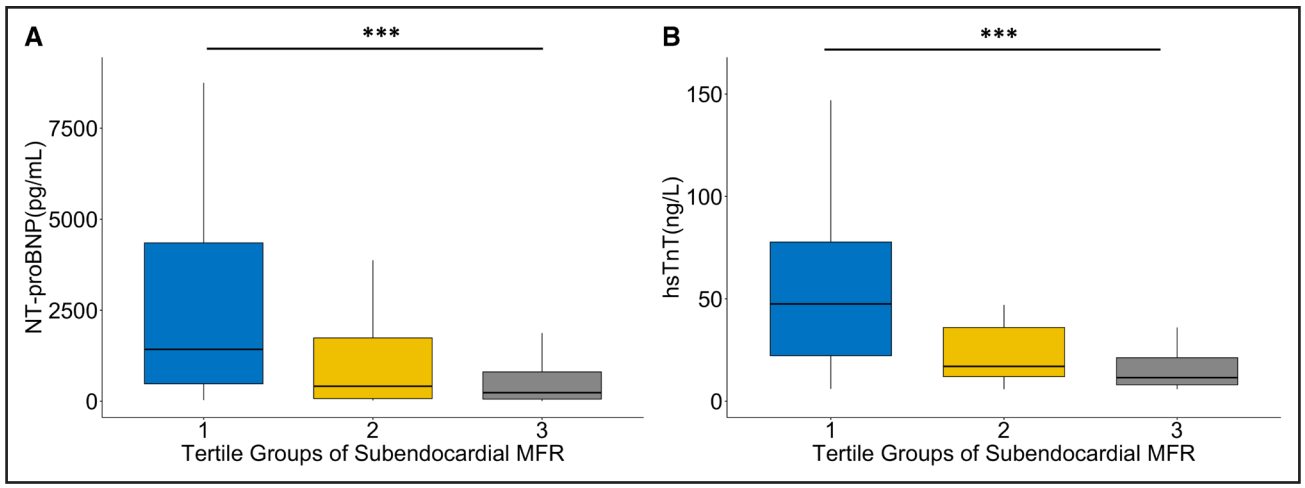

Figure 2. Association between subendocardial myocardial flow reserve and myocardial stress and injury.
The stepwise relationship of lower subendocardial flow reserve with more severe myocardial stress (NT-proBNP, **A**) and injury (hsTnT, **B**) is shown. ***$P<0.001$. hsTnT indicates high-sensitivity cardiac troponin T; $MFR_{subendo}$, subendocardial myocardial flow reserve; and NT-proBNP, N-terminal pro-B-type natriuretic peptide.

and renal dysfunction, as well as with markers of myocardial injury and more adverse LV structural parameters, independent of cardiovascular risk factors and atherosclerotic burden. Importantly, lower $MFR_{subendo}$ was associated with worse prognosis, including increased rates of all-cause death and HF hospitalization. Thus, PET quantification of subendocardial perfusion and MFR captures a relevant marker of pathophysiology and cardiovascular risk. Given the importance of coronary microvascular dysfunction in hypertension and HF, and the predisposition of the subendocardium to ischemia, we herein extend evidence of the feasibility of PET quantification of subendocardial blood flow and MFR to show its pathophysiologic and prognostic relevance in the absence of flow-limiting epicardial CAD. Future studies should examine whether $MFR_{subendo}$ can provide additive information to transmural flow reserve in populations at especially high risk of subendocardial ischemia and HF.

In the absence of obstructive epicardial CAD, coronary microvascular dysfunction and diffuse atherosclerosis are central determinants of angina and ischemia, are common in patients with hypertension and other adverse metabolic states, and have been associated with increased HF risk.[25–29] The subendocardium is particularly vulnerable to microvascular ischemia because of multiple contributors, both those reducing myocardial oxygen supply and those increasing myocardial oxygen demand.[30] Various animal experiments have demonstrated the early appearance of subendocardial hypoperfusion and dysfunction in models of LV hypertrophy,[31,32] and impairment in perfusion to the subendocardium has been identified in humans with hypertension, aortic stenosis, hypertrophic cardiomyopathy, and chronic kidney disease.[10–12,33,34] In patients with severe aortic stenosis evaluated by ^{15}O-H_2O PET, there was evidence of impaired hyperemic subendocardial blood flow that increased in severity with the severity of aortic stenosis and hemodynamic load.[10] In patients with hypertrophic cardiomyopathy with normal epicardial coronary arteries, augmentation of hyperemic blood flow in the subendocardium has been demonstrated to be substantially reduced, corresponding to the degree of wall thickness[11] and to the presence of ischemic cavity dilatation,[12] implicating both anatomic and hemodynamic causes. In our study, we similarly demonstrated that more impaired subendocardial perfusion was associated with higher NT-proBNP, indicative of higher wall stress, and with greater wall thickness, LV mass, and chamber volumes, suggesting possible early subclinical indicators of adverse structural remodeling.

Although previous studies in states of pathologic hypertrophy have quantified impairment in subendocardial perfusion,[10–12] alterations in subendocardial perfusion have not previously been shown to predict adverse outcomes. One previous study has evaluated prognosis in patients referred for stress testing with isolated abnormalities in subendocardial perfusion by ^{82}Rubidium PET and did not find any adverse impact on the rate of atherosclerotic events,[35] although it did not include assessment of HF, a relevant outcome given the relationships demonstrated herein between subendocardial MFR and cardiac structure and injury. We demonstrated that lower $MFR_{subendo}$ was independently associated with increased rates of composite cardiac and cerebrovascular events as well as with an increased rate of HF hospitalization. Like transmural MFR, subendocardial flow reserve was a valid physiologic metric that captured not only physiologic but prognostically relevant impairments of vasomotor function.

From a technical standpoint, one could worry that PET-based estimates of subendocardial perfusion, especially those derived from ventricles with normal wall

Downloaded from http://ahajournals.org by on March 29, 2025

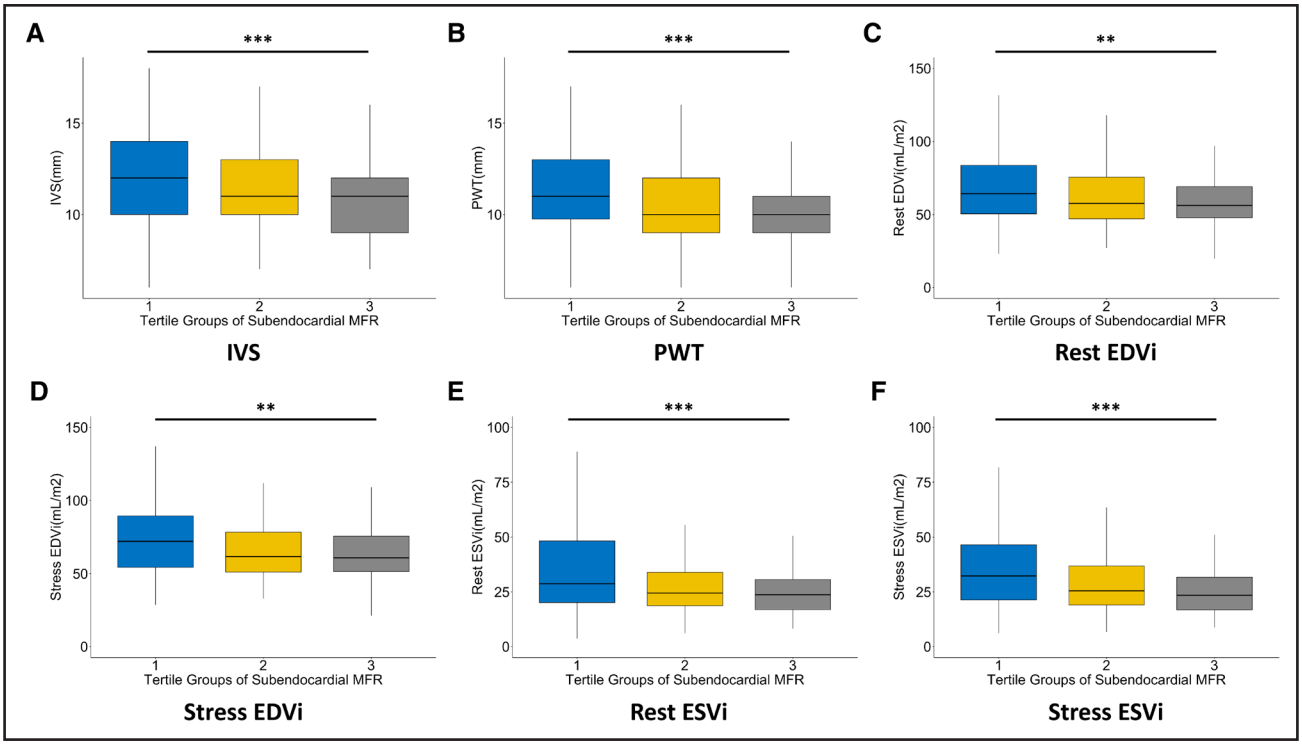

Figure 3. Association between subendocardial myocardial flow reserve and left ventricular structure.
Lower subendocardial flow reserve demonstrated a stepwise relationship with more adverse chamber dimensions including higher interventricular septal (**A**) and posterior wall thickness (**B**) and greater end-diastolic and end-systolic dimensions at rest (**C** and **E**) and stress (**D** and **F**). $^{**}P<0.01$. $^{***}P<0.001$. EDVi indicates end-diastolic volume indexed to body surface area; ESVi, end-systolic volume indexed to body surface area; IVS, interventricular septal wall thickness; and PWT, posterior wall thickness.

thickness, would be potentially inaccurate because of partial volume and spillover effects. However, previous studies in experimental animals[36] and in humans with and without discrete epicardial stenoses[9,37] have shown the ability to reliably ascertain subendocardial blood flow, as distinct from subepicardial perfusion, in the absence of pathologic hypertrophy. The current study further provides substantive evidence of the reliability of quantification of subendocardial blood flow and MFR in patients with generally normal wall thickness by demonstrating the relationship of $MFR_{subendo}$ to relevant comorbidities, atherosclerotic burden, cardiac structure and biomarkers, and clinical outcomes.

Despite the vulnerability of the subendocardium to ischemic injury, no difference between transmural MFR and $MFR_{subendo}$ could be detected in our study, and we do not demonstrate that $MFR_{subendo}$ was additive to transmural MFR in predicting clinical outcomes. We hypothesize this may be a result of the included population being "too healthy," with largely normal LV wall thickness and thus likely relatively mild absolute subendocardial hypoperfusion. Therefore, we suspect that patients with overt LV remodeling or LV hypertrophy, like those with hypertrophic cardiomyopathy or advanced chronic kidney disease, may have more discrepant subendocardial versus transmural perfusion, and investigation of the value of

Table 3. Association of Subendocardial MFR With Cardiac Injury

Cardiac biomarkers	Comparison	Unadjusted odds ratio (95% CI)	*P* value	Adjusted* odds ratio (95% CI)	*P* value	Adjusted† odds ratio (95% CI)	*P* value
Elevated NT-proBNP	Tertile 1 vs 3	4.33 (2.09 to 9.26)	<0.001	2.69 (1.20 to 6.15)	0.017	2.64 (1.17 to 6.08)	0.021
	Tertile 2 vs 3	1.21 (0.60 to 2.44)	0.60	1.10 (0.51 to 2.35)	0.81	1.08 (0.50 to 2.33)	0.84
Elevated hsTnT	Tertile 1 vs 3	7.42 (3.14 to 18.59)	<0.001	3.18 (1.11 to 9.38)	0.033	2.56 (0.86 to 7.77)	0.091
	Tertile 2 vs 3	1.91 (0.84 to 4.47)	0.127	1.39 (0.52 to 3.81)	0.51	1.17 (0.42 to 3.30)	0.76

Lower subendocardial MFR was independently associated with higher risk of myocardial injury in multivariable regression models comparing the lowest with the highest tertile group. NT-proBNP n=209, hsTnT n=155. hsTnT indicates high-sensitivity cardiac troponin T; MFR, myocardial flow reserve; and NT-proBNP, N-terminal pro-B-type natriuretic peptide.

*Adjusted for age, sex, diabetes, and estimated glomerular filtration rate.

†In addition, adjusted for qualitative coronary calcium score (CAC).

Downloaded from http://ahajournals.org by on March 29, 2025

Table 4. Association of Subendocardial MFR With Cardiac Structure

Cardiac structure	Comparison	Unadjusted mean difference (95% CI)	*P* value	Adjusted* mean difference (95% CI)	*P* value	Adjusted† mean difference (95% CI)	*P* value
LVEF, %	Tertile 1 vs 3	−3.48 (−6.91 to −0.04)	0.048	−2.90 (−6.68 to 0.89)	0.13	−3.68 (−7.46 to 0.11)	0.057
	Tertile 2 vs 3	−1.23 (−4.66 to 2.20)	0.48	−1.38 (−4.95 to −2.19)	0.45	−1.65 (−5.19 to −1.89)	0.36
E/A	Tertile 1 vs 3	2.43 (−1.22 to 6.09)	0.19	2.40 (−1.76 to 6.55)	0.26	2.18 (−2.02 to 6.38)	0.31
	Tertile 2 vs 3	−0.10 (−3.72 to 3.51)	0.96	−0.10 (−3.9 to 3.78)	0.96	−0.16 (−4.04 to 3.73)	0.94
IVS, mm	Tertile 1 vs 3	1.24 (0.62 to 1.86)	<0.001	0.86 (0.20 to 1.53)	0.011	0.89 (0.21 to 1.56)	0.010
	Tertile 2 vs 3	0.66 (0.05 to 1.28)	0.036	0.41 (−0.21 to 1.04)	0.20	0.42 (−0.21 to 1.05)	0.19
PWT, mm	Tertile 1 vs 3	1.37 (0.84 to 1.91)	<0.001	1.21 (0.63 to 1.79)	<0.001	1.22 (0.64 to 1.81)	<0.001
	Tertile 2 vs 3	0.20 (−0.34 to 0.73)	0.47	0.19 (−0.36 to 0.73)	0.50	0.19 (−0.35 to 0.74)	0.49
Rest EDVi, mL/m^2	Tertile 1 vs 3	9.19 (−0.30 to 18.67)	0.058	10.60 (0.36 to 20.84)	0.043	12.37 (2.09 to 22.66)	0.018
	Tertile 2 vs 3	1.14 (−8.41 to 10.69)	0.82	3.02 (−6.68 to 12.72)	0.54	3.44 (−6.20 to 13.09)	0.48
Stress EDVi, mL/m^2	Tertile 1 vs 3	12.71 (4.85 to 20.58)	0.002	13.24 (4.85 to 21.63)	0.002	14.24 (5.77 to 22.72)	0.001
	Tertile 2 vs 3	3.10 (−4.78 to 10.98)	0.44	4.89 (−3.06 to 12.84)	0.23	5.17 (−2.77 to 13.12)	0.20
Rest ESVi, mL/m^2	Tertile 1 vs 3	11.86 (4.72 to 18.99)	0.001	10.98 (3.26 to 18.70)	0.005	12.42 (4.67 to 20.16)	0.002
	Tertile 2 vs 3	4.13 (−3.05 to 11.31)	0.26	4.73 (−2.58 to 12.04)	0.20	5.07 (−2.19 to 12.33)	0.17
Stress ESVi, mL/m^2	Tertile 1 vs 3	11.57 (4.55 to 18.59)	0.001	10.48 (2.88 to 18.09)	0.007	11.70 (4.04 to 19.36)	0.003
	Tertile 2 vs 3	2.81 (−4.23 to 9.84)	0.43	3.49 (−3.72 to 10.70)	0.34	3.83 (−3.36 to 11.01)	0.30
LVMI, g/m^2	Tertile 1 vs 3	9.24 (4.42 to 14.06)	<0.001	9.03 (3.75 to 14.31)	<0.001	9.38 (4.02 to 14.73)	0.001
	Tertile 2 vs 3	1.88 (−2.97 to 6.73)	0.45	2.51 (−2.53 to 7.54)	0.33	2.62 (−2.42 to 7.67)	0.31

Lower subendocardial MFR was independently associated with greater left ventricular wall thickness and mass, and larger left ventricular volumes in multivariable regression models comparing the lowest with the highest tertile group. LVEF n=354, E/A n=310.

EDVi indicates end-diastolic volume index; ESVi, end-systolic volume index; IVS, interventricular septum; LVEF, left ventricular ejection fraction; LVMI, left ventricular mass index; MFR, myocardial flow reserve; and PWT, posterior wall thickness.

*Adjusted for age, sex, diabetes, and estimated glomerular filtration rate.

†In addition, adjusted for qualitative coronary calcium score (CAC).

Downloaded from http://ahajournals.org by on March 29, 2025

subendocardial perfusion assessment when transmural MFR is normal would be worthwhile to explore with this technique in future studies, because the perfusion of subendocardium may be far more impaired secondary to extracellular matrix accumulation and myocardial fibrosis in these patients.[38]

Strengths and Limitations

This study has the benefit of state-of-the-art dynamic physiologic imaging and follow-up for highly relevant clinical events including HF. However, several limitations need attention. First, this is a single-center study of a clinical referral population and may not be widely generalizable to other centers, and cardiac biomarkers and echocardiograms were obtained on a clinical basis rather than prospectively ordered for research. Second, as above, because of limitations on spatial resolution, we define the subendocardium as the inner half of the LV wall, which likely contains central myocardial layers as well, and the "spillover" effect may lead to the overestimation of $MFR_{subendo}$ and dilute the differences detected between $MFR_{subendo}$ and transmural MFR. However, the kinetic modeling algorithm used to quantify myocardial blood flow minimizes partial volume effects by estimating the spillover fraction as an adjustable model parameter. Furthermore, despite potential overestimation, lower $MFR_{subendo}$ was consistently associated with more adverse cardiac chamber dimensions, cardiac biomarkers, and clinical events, suggesting it is capturing biologically relevant subendocardial ischemia. Third, because the assessment of subendocardial blood flow is not in widespread use, there are not established normal values and expected distributions, and the use of tertiles, rather than other quantiles or continuous distribution, has known limitations; however, $MFR_{subendo}$ was associated with adverse structure and events across low, intermediate, and high tertile groups rather than being dependent on a specific or arbitrary abnormal threshold. Fourth, because the inclusion criteria restricted the study to a relatively healthy population with normal perfusion, the frequency of severely impaired MFR was low, and we were not able to demonstrate superior sensitivity of $MFR_{subendo}$ compared with transmural MFR in predicting clinical prognosis. Moreover, we observed relatively few clinical events, particularly for MI and stroke, which limited statistical power for these analyses. Nonetheless, $MFR_{subendo}$ captured a meaningful pathophysiologic and prognostic parameter, and whether it could provide additive value to transmural flow reserve to warrant its eventual clinical use in certain higher risk populations is worthy of additional study. Last, E/A ratio is a very

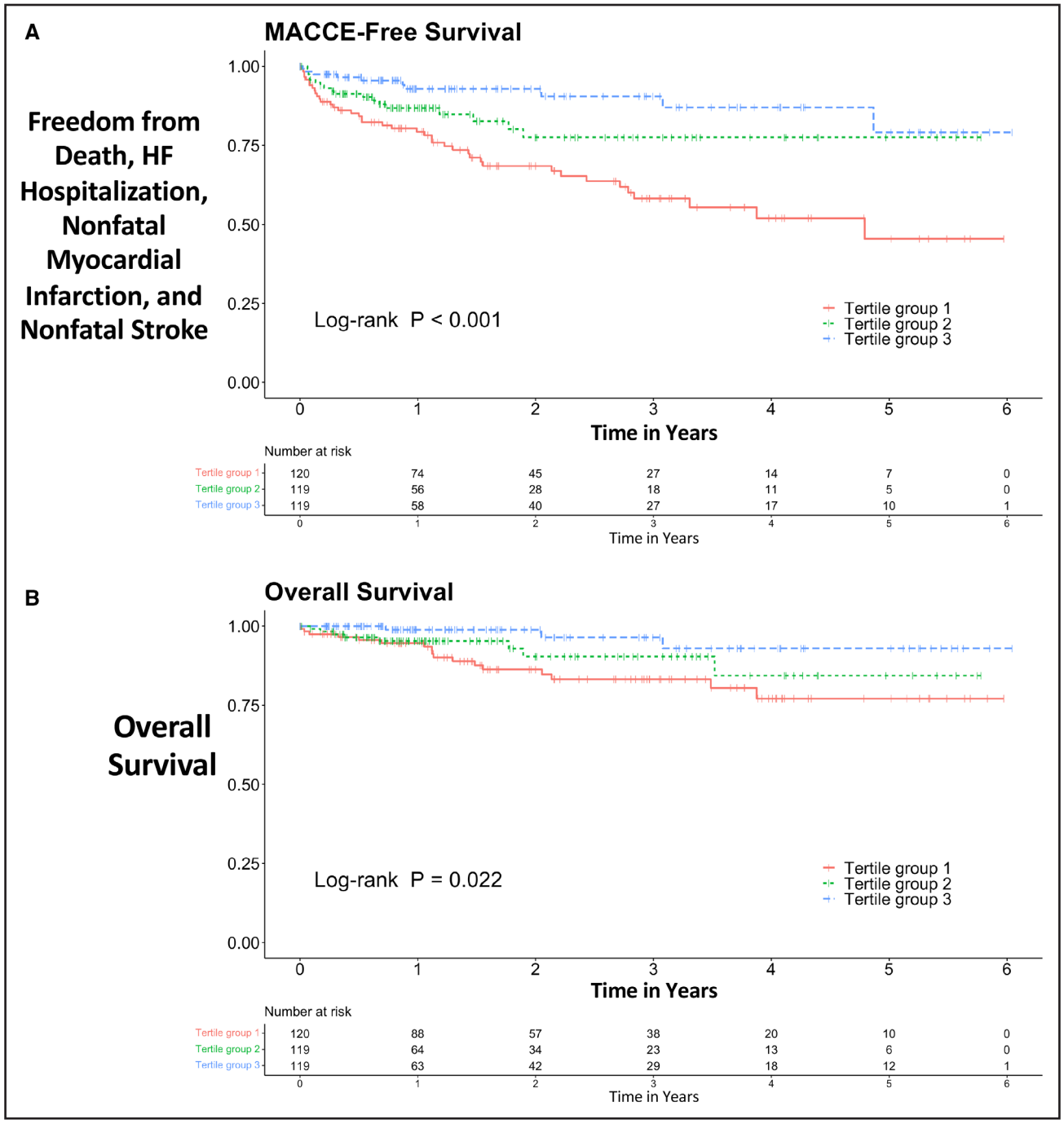

Figure 4. Event-free survival by tertile of subendocardial myocardial flow reserve.
The Kaplan-Meier curves for MACCE (**A**) and overall survival (**B**) according to tertile group of subendocardial flow reserve are shown. Lower tertile of subendocardial MFR indicated worse long-term prognosis. HF indicates heart failure; MACCE, major adverse cardiac and cerebrovascular events (all-cause death, HF hospitalization, nonfatal myocardial infarction, nonfatal stroke); and MFR, myocardial flow reserve.

imperfect measure of diastolic function that declines in milder diastolic dysfunction and then rises as severity of diastolic dysfunction increases. Dedicated studies to link subendocardial perfusion to comprehensive diastolic function assessment would be valuable in further proving the hypothesized relationship between subendocardial ischemia, fibrosis, and HF among patients with hypertension.

CONCLUSIONS

In this study, reduced subendocardial perfusion was closely associated with increased cardiovascular risk factors, myocardial injury, adverse LV structural parameters, and MACCE, independent of traditional risk factors and the burden of atherosclerosis. Although not independent of transmural MFR, $MFR_{subendo}$ was reliably quantified

Downloaded from http://ahajournals.org by on March 29, 2025

Table 5. Association Between Subendocardial MFR and Clinical Outcomes

Cox regression	N events	Comparison	Unadjusted HR (95% CI)	*P* value	Adjusted HR* (95% CI)	*P* value	Adjusted HR† (95% CI)	*P* value
Primary outcome								
MACCE	69	Tertile 1 vs 3	4.09 (2.05–8.16)	<0.001	3.90 (1.84–8.27)	<0.001	2.99 (1.39–6.44)	0.005
		Tertile 2 vs 3	2.07 (0.95–4.49)	0.07	1.97 (0.89–4.36)	0.09	1.61 (0.72–3.61)	0.25
Secondary outcomes								
MACE	61	Tertile 1 vs 3	3.99 (1.93–8.28)	<0.001	3.48 (1.57–7.71)	0.002	2.66 (1.19–5.97)	0.017
		Tertile 2 vs 3	1.84 (0.81–4.21)	0.15	1.67 (0.72–3.91)	0.23	1.33 (0.56–3.16)	0.52
All-cause death	28	Tertile 1 vs 3	4.79 (1.40–16.35)	0.013	3.36 (0.90–12.52)	0.071	2.71 (0.71–10.34)	0.15
		Tertile 2 vs 3	2.99 (0.79–11.27)	0.11	2.45 (0.65–9.46)	0.19	2.04 (0.52–7.99)	0.31
Heart failure hospitalization	38	Tertile 1 vs 3	4.05 (1.66–9.88)	0.002	3.61 (1.36–9.55)	0.010	2.76 (1.04–7.32)	0.042
		Tertile 2 vs 3	1.25 (0.4–3.72)	0.69	1.12 (0.37–3.43)	0.84	0.84 (0.26–2.69)	0.77
Nonfatal MI	4	Tertile 1 vs 3	2.01 (0.18–22.30)	0.57	1.13 (0.08–16.53)	0.93	0.37 (0.02–8.69)	0.54
		Tertile 2 vs 3	1.16 (0.07–18.68)	0.92	0.75 (0.04–13.11)	0.84	0.64 (0.03–12.29)	0.77
Nonfatal stroke	12	Tertile 1 vs 3	2.28 (0.44–11.76)	0.33	2.56 (0.43–15.11)	0.30	1.84 (0.29–11.79)	0.52
		Tertile 2 vs 3	2.92 (0.57 –15.08)	0.20	2.94 (0.54–16.09)	0.21	2.55 (0.45–14.45)	0.29

Data are hazard ratios and associated 95% CIs from Cox regression models for time to first MACCE event, time to first MACE event, and time to all-cause death. Data are cause-specific hazard ratio from cause-specific proportional hazards models for time to nonfatal stroke, time to nonfatal MI, and time to heart failure hospitalization. The highest tertile group 3 is set as the reference. HR indicates hazard ratio; MACCE, major adverse cardiac and cerebrovascular event; MACE, major adverse cardiovascular event; and MI, myocardial infarction.

*Adjusted for age, sex, diabetes, estimated glomerular filtration rate, and coronary calcium score.

†In addition, adjusted for mean left ventricular wall thickness and left ventricular ejection fraction.

and associated with structural and prognostic outcomes. In patients with hypertension and hypertrophy who are at risk for subendocardial ischemia out of proportion to transmural impairments in blood flow, $MFR_{subendo}$ may be a promising tool for exploring the pathophysiology of hypertensive heart disease and HF.

ARTICLE INFORMATION

Received September 11, 2023; accepted July 29, 2024.

Affiliations

Zhejiang University School of Medicine, Hangzhou, China (X.X., L.Z.). Cardiovascular Imaging Program, Departments of Medicine and Radiology (X.X., S. Divakaran, B.N.W., J.H., S.S.L., B.A., M.F.K., R.B., S. Dorbala, J.M.B., M.F.D.C.), Heart and Vascular Center, Division of Cardiovascular Medicine, Department of Medicine (S. Divakaran, B.N.W., R.B., J.M.B., M.F.D.C.), Brigham and Women's Hospital, Harvard Medical School, Boston, MA. Department of Cardiology, and Institute for Developmental and Regenerative Cardiovascular Medicine, Xinhua Hospital Affiliated to Shanghai Jiaotong University School of Medicine, Shanghai, China (X.X., L.Z.). Institute for Clinical Research and Health Policy Studies, Tufts Medical Center, Boston, MA (L.T.). Tufts Clinical and Translational Science Institute, Tufts University, Boston, MA (L.T.). Division of Artificial Intelligence, Department of Medicine, Cedars-Sinai, Los Angeles, CA (P.S.).

Sources of Funding

X.X. is supported by the Sarnoff Cardiovascular Research Foundation. B.W. is supported by an American Heart Association Career Development Award (21CDA851511) and the National Institutes of Health/National Heart, Lung, and Blood Institute K23 award (K23HL159276). S. Dorbala is supported by the National Institutes of Health/National Heart, Lung, and Blood Institute K24 award (K24HL157648). L.Z. is supported by the National Science Fund for Distinguished Young Scholars of China (82125005). J.M.B. is supported by an American Heart Association Career Development Award (21CDA852429) and the National Institutes of Health/National Heart, Lung, and Blood Institute K23 award (K23HL159279). This work is supported in part by National Institutes of Health/National Heart, Lung, and Blood Institute grants T32 HL094301 (M.F.D.C., S. Divakaran, B.W.) and R01EB034586 (P.J.S., M.F.D.C.). All work with QPET was performed at Brigham and Women's Hospital (analysis) and Cedars-Sinai (algorithm development).

Disclosures

B.W. reports consulting fees from Horizon Therapeutics, Kiniksa Pharmaceuticals, and Novo Nordisk. B.A. reports consulting fees from Spectrum Dynamics Medical. S. Dorbala reports grant support from Attralus, Pfizer, GE Healthcare, Phillips, and Siemens; S. Dorbala has consulted with Novo Nordisk and Alexion. R.B. reports research support from Amgen and Novartis and has consulted for Caristo Inc and Elucid Inc. P.J.S. reports consulting fees from Synektik, SA, research support from Siemens, and software royalties from Cedars-Sinai licensing. J.M.B. reports consulting fees from Bayer AG and AstraZeneca. M.F.D.C. reports grant support from Gilead Sciences, in-kind research support from Amgen, and consulting fees from MedTrace and Sanofi. The other authors report no conflicts.

Supplemental Material

Tables S1–S5

Figures S1 and S2

REFERENCES

1. Camici PG, Tschöpe C, Di Carli MF, Rimoldi O, Van Linthout S. Coronary microvascular dysfunction in hypertrophy and heart failure. *Cardiovasc Res*. 2020;116:806–816. doi: 10.1093/cvr/cvaa023
2. Shah SJ, Lam CSP, Svedlund S, Saraste A, Hage C, Tan RS, Beussink-Nelson L, Ljung Faxén U, Fermer ML, Broberg MA, et al. Prevalence and correlates of coronary microvascular dysfunction in heart failure with preserved ejection fraction: PROMIS-HFpEF. *Eur Heart J*. 2018;39:3439–3450. doi: 10.1093/eurheartj/ehy531
3. Zhou W, Brown JM, Bajaj NS, Chandra A, Divakaran S, Weber B, Bibbo CF, Hainer J, Taqueti VR, Dorbala S, et al. Hypertensive coronary microvascular dysfunction: a subclinical marker of end organ damage and heart failure. *Eur Heart J*. 2020;41:2366–2375. doi: 10.1093/eurheartj/ehaa191
4. Shenasa M, Shenasa H, El-Sherif N. Left ventricular hypertrophy and arrhythmogenesis. *Card Electrophysiol Clin*. 2015;7:207–220. doi: 10.1016/j.ccep.2015.03.017
5. Feher A, Sinusas AJ. Quantitative assessment of coronary microvascular function: dynamic single-photon emission computed tomography, positron emission tomography, ultrasound, computed tomography, and magnetic

Downloaded from http://ahajournals.org by on March 29, 2025

resonance imaging. *Circ Cardiovasc Imaging*. 2017;10:e006427. doi: 10.1161/CIRCIMAGING.117.006427
6. Schindler TH, Fearon WF, Pelletier-Galarneau M, Ambrosio G, Sechtem U, Ruddy TD, Patel KK, Bhatt DL, Bateman TM, Gewirtz H, et al. Myocardial perfusion PET for the detection and reporting of coronary microvascular dysfunction: a JACC: Cardiovascular Imaging Expert Panel statement. *JACC Cardiovasc Imaging*. 2023;16:536–548. doi: 10.1016/j.jcmg.2022.12.015
7. Levy BI, Heusch G, Camici PG. The many faces of myocardial ischaemia and angina. *Cardiovasc Res*. 2019;115:1460–1470. doi: 10.1093/cvr/cvz160
8. Gould KL, Nguyen T, Kirkeeide R, Roby AE, Bui L, Kitkungvan D, Patel MB, Madjid M, Haynie M, Lai D, et al. Subendocardial and transmural myocardial ischemia: clinical characteristics, prevalence, and outcomes with and without revascularization. *JACC Cardiovasc Imaging*. 2023;16:78–94. doi: 10.1016/j.jcmg.2022.05.016
9. Vermeltfoort IA, Raijmakers PG, Lubberink M, Germans T, van Rossum AC, Lammertsma AA, Knaapen P. Feasibility of subendocardial and subepicardial myocardial perfusion measurements in healthy normals with (15)O-labeled water and positron emission tomography. *J Nucl Cardiol*. 2011;18:650–656. doi: 10.1007/s12350-011-9375-y
10. Rajappan K, Rimoldi OE, Dutka DP, Ariff B, Pennell DJ, Sheridan DJ, Camici PG. Mechanisms of coronary microcirculatory dysfunction in patients with aortic stenosis and angiographically normal coronary arteries. *Circulation*. 2002;105:470–476. doi: 10.1161/hc0402.102931
11. Knaapen P, Germans T, Camici PG, Rimoldi OE, ten Cate FJ, ten Berg JM, Dijkmans PA, Boellaard R, van Dockum WG, Götte MJ, et al. Determinants of coronary microvascular dysfunction in symptomatic hypertrophic cardiomyopathy. *Am J Physiol Heart Circ Physiol*. 2008;294:H986–H993. doi: 10.1152/ajpheart.00233.2007
12. Yalçin H, Valenta I, Yalçin F, Corona-Villalobos C, Vasquez N, Ra J, Kucukler N, Tahari A, Pozios I, Zhou Y, et al. Effect of diffuse subendocardial hypoperfusion on left ventricular cavity size by (13)N-ammonia perfusion PET in patients with hypertrophic cardiomyopathy. *Am J Cardiol*. 2016;118:1908–1915. doi: 10.1016/j.amjcard.2016.08.085
13. Danad I, Raijmakers PG, Driessen RS, Leipsic J, Raju R, Naoum C, Knuuti J, Mäki M, Underwood RS, Min JK, et al. Comparison of coronary CT angiography, SPECT, PET, and hybrid imaging for diagnosis of ischemic heart disease determined by fractional flow reserve. *JAMA Cardiol*. 2017;2:1100–1107. doi: 10.1001/jamacardio.2017.2471
14. Cerqueira MD, Weissman NJ, Dilsizian V, Jacobs AK, Kaul S, Laskey WK, Pennell DJ, Rumberger JA, Ryan T, Verani MS; American Heart Association Writing Group on Myocardial Segmentation and Registration for Cardiac Imaging. Standardized myocardial segmentation and nomenclature for tomographic imaging of the heart. A statement for healthcare professionals from the Cardiac Imaging Committee of the Council on Clinical Cardiology of the American Heart Association. *Circulation*. 2002;105:539–542. doi: 10.1161/hc0402.102975
15. Fang M, Wang D, Tang O, McEvoy JW, Echouffo-Tcheugui JB, Christenson RH, Selvin E. Subclinical cardiovascular disease in US adults with and without diabetes. *J Am Heart Assoc*. 2023;12:e029083. doi: 10.1161/JAHA.122.029083
16. Kim HN, Januzzi JL Jr. Natriuretic peptide testing in heart failure. *Circulation*. 2011;123:2015–2019. doi: 10.1161/CIRCULATIONAHA.110.979500
17. Inker LA, Eneanya ND, Coresh J, Tighiouart H, Wang D, Sang Y, Crews DC, Doria A, Estrella MM, Froissart M, et al; Chronic Kidney Disease Epidemiology Collaboration. New creatinine- and cystatin C-based equations to estimate GFR without race. *N Engl J Med*. 2021;385:1737–1749. doi: 10.1056/NEJMoa2102953
18. Slomka PJ, Alexanderson E, Jácome R, Jiménez M, Romero E, Meave A, Le Meunier L, Dalhbom M, Berman DS, Germano G, et al. Comparison of clinical tools for measurements of regional stress and rest myocardial blood flow assessed with 13N-ammonia PET/CT. *J Nucl Med*. 2012;53:171–181. doi: 10.2967/jnumed.111.095398
19. Chiles C, Duan F, Gladish GW, Ravenel JG, Baginski SG, Snyder BS, DeMello S, Desjardins SS, Munden RF; NLST Study Team. Association of coronary artery calcification and mortality in the National Lung Screening Trial: a comparison of three scoring methods. *Radiology*. 2015;276:82–90. doi: 10.1148/radiol.15142062
20. Einstein AJ, Johnson LL, Bokhari S, Son J, Thompson RC, Bateman TM, Hayes SW, Berman DS. Agreement of visual estimation of coronary artery calcium from low-dose CT attenuation correction scans in hybrid PET/CT and SPECT/CT with standard Agatston score. *J Am Coll Cardiol*. 2010;56:1914–1921. doi: 10.1016/j.jacc.2010.05.057
21. Thygesen K, Alpert JS, Jaffe AS, Chaitman BR, Bax JJ, Morrow DA, White HD; ESC Scientific Document Group. Fourth universal definition of myocardial infarction (2018). *Eur Heart J*. 2019;40:237–269. doi: 10.1093/eurheartj/ehy462
22. Yew KS, Cheng E. Acute stroke diagnosis. *Am Fam Physician*. 2009;80:33–40.
23. Bajaj NS, Osborne MT, Gupta A, Tavakkoli A, Bravo PE, Vita T, Bibbo CF, Hainer J, Dorbala S, Blankstein R, et al. Coronary microvascular dysfunction and cardiovascular risk in obese patients. *J Am Coll Cardiol*. 2018;72:707–717. doi: 10.1016/j.jacc.2018.05.049
24. Austin PC, Lee DS, Fine JP. Introduction to the analysis of survival data in the presence of competing risks. *Circulation*. 2016;133:601–609. doi: 10.1161/CIRCULATIONAHA.115.017719
25. Feihl F, Liaudet L, Levy BI, Waeber B. Hypertension and microvascular remodelling. *Cardiovasc Res*. 2008;78:274–285. doi: 10.1093/cvr/cvn022
26. Bajaj N, Singh A, Zhou W, Gupta A, Fujikura K, Byrne C, Harms HJ, Osborne MT, Bravo P, Andrikopoulou E, et al. Coronary microvascular dysfunction, left ventricular remodeling and clinical outcomes in patients with chronic kidney impairment. *Circulation*. 2020;141:21–33.
27. Rush CJ, Berry C, Oldroyd KG, Rocchiccioli JP, Lindsay MM, Touyz RM, Murphy CL, Ford TJ, Sidik N, McEntegart MB, et al. Prevalence of coronary artery disease and coronary microvascular dysfunction in patients with heart failure with preserved ejection fraction. *JAMA Cardiol*. 2021;6:1130–1143. doi: 10.1001/jamacardio.2021.1825
28. Arnold JR, Kanagala P, Budgeon CA, Jerosch-Herold M, Gulsin GS, Singh A, Khan JN, Chan DCS, Squire IB, Ng LL, et al. Prevalence and prognostic significance of microvascular dysfunction in heart failure with preserved ejection fraction. *JACC Cardiovasc Imaging*. 2022;15:1001–1011. doi: 10.1016/j.jcmg.2021.11.022
29. Taqueti VR, Solomon SD, Shah AM, Desai AS, Groarke JD, Osborne MT, Hainer J, Bibbo CF, Dorbala S, Blankstein R, et al. Coronary microvascular dysfunction and future risk of heart failure with preserved ejection fraction. *Eur Heart J*. 2018;39:840–849. doi: 10.1093/eurheartj/ehx721
30. Algranati D, Kassab GS, Lanir Y. Why is the subendocardium more vulnerable to ischemia? A new paradigm. *Am J Physiol Heart Circ Physiol*. 2011;300:H1090–H1100. doi: 10.1152/ajpheart.00473.2010
31. Nakano K, Corin WJ, Spann JF Jr., Biederman RW, Denslow S, Carabello BA. Abnormal subendocardial blood flow in pressure overload hypertrophy is associated with pacing-induced subendocardial dysfunction. *Circ Res*. 1989;65:1555–1564. doi: 10.1161/01.res.65.6.1555
32. Hittinger L, Shen YT, Patrick TA, Hasebe N, Komamura K, Ihara T, Manders WT, Vatner SF. Mechanisms of subendocardial dysfunction in response to exercise in dogs with severe left ventricular hypertrophy. *Circ Res*. 1992;71:423–434. doi: 10.1161/01.res.71.2.423
33. Ekart R, Bevc S, Hojs N, Hojs R. Derived subendocardial viability ratio and cardiovascular events in patients with chronic kidney disease. *Cardiorenal Med*. 2019;9:41–50. doi: 10.1159/000493512
34. Amah G, Ouardani R, Pasteur-Rousseau A, Voicu S, Safar ME, Kubis N, Bonnin P. Extreme-dipper profile, increased aortic stiffness, and impaired subendocardial viability in hypertension. *Am J Hypertens*. 2017;30:417–426. doi: 10.1093/ajh/hpw209
35. Gould KL, Nguyen T, Kirkeeide R, Roby AE, Bui L, Kitkungvan D, Patel MB, Madjid M, Haynie M, Lai D, et al. Subendocardial and transmural myocardial ischemia: clinical characteristics, prevalence, and outcomes with and without revascularization. *JACC Cardiovasc Imaging*. 2022;16:78–94. doi: 10.1016/j.jcmg.2022.05.016
36. Rimoldi O, Schäfers KP, Boellaard R, Turkheimer F, Stegger L, Law MP, Lammerstma AA, Camici PG. Quantification of subendocardial and subepicardial blood flow using 15O-labeled water and PET: experimental validation. *J Nucl Med*. 2006;47:163–172.
37. Danad I, Raijmakers PG, Harms HJ, Heymans MW, van Royen N, Lubberink M, Boellaard R, van Rossum AC, Lammertsma AA, Knaapen P. Impact of anatomical and functional severity of coronary atherosclerotic plaques on the transmural perfusion gradient: a [15O]H2O PET study. *Eur Heart J*. 2014;35:2094–2105. doi: 10.1093/eurheartj/ehu170
38. Aguiar Rosa S, Rocha Lopes L, Fiarresga A, Ferreira RC, Mota Carmo M. Coronary microvascular dysfunction in hypertrophic cardiomyopathy: pathophysiology, assessment, and clinical impact. *Microcirculation*. 2021;28:e12656. doi: 10.1111/micc.12656

Downloaded from http://ahajournals.org by on March 29, 2025